

Nodal prices determination with wind integration for radial distribution system

Manish Kumar¹, Karimulla Piolliseti², Ashwani Kumar^{3*}, K.S. Sandhu⁴

^{1,2,3,4}Department of Electrical Engineering, National Institute of Technology Kurukshetra, INDIA
^{*}Corresponding Author: e-mail: ashwani.k.sharma@nitkr.ac.in, Tel.: +911744233389; fax: +911744238050

Abstract

With competitive electricity market operation, open access to the transmission and distribution network is essential for transparent and efficient market operation. Like transmission pricing, distribution network pricing must also be transparent and must include time variations based on the change in the operating state of the system, integration of renewable sources and must be real time. In this paper, a distribution system nodal pricing scheme is proposed for radial distribution system with integration of wind power in the system. The main objective of the paper is: (i) an optimal power flow based approach for determination of nodal prices for distribution system, (ii) impact of wind generation on nodal prices. The results have been obtained for IEEE 33 bus test system.

Keywords: Distribution system, electricity market; nodal prices, wind power integration.

DOI: <http://dx.doi.org/10.4314/ijest.v9i3.2>

1. Introduction

Competitive electricity market sustainability and market efficiency is dependent on the transparent pricing structure. It is observed that the techniques used for the transmission pricing can also be applied to the distribution system such as nodal pricing, which is an efficient method for calculation of marginal cost of energy along with marginal cost of losses (Ghayeni and Ghazi, 2011). A dispersed generation is considered to allocate the losses using marginal loss coefficients and direct loss coefficients to determine the nodal prices in Mutale et al. (2000). Renewable energy sources have become essential part of the distribution network due to environmental constraints and regulatory policies worldwide. and it is essential to determine their impact on the prices at the nodes. Authors in Zhao et al. (2011) studied the impact of renewable energy integration on nodal prices considering the effect of intermittent load. Nodal pricing based method is also used for the location of DG as discussed in (Singh and Goswami (2006)). The analysis presented in Singh and Goswami (2006) is applied for loss minimization in Sotkiewicz and Vignolo (2006). In Zhao (2010) as well as Sotkiewicz and Vignolo (2012), the effect of solar and wind generation on distribution system prices were analyzed. The dynamic tariff concept is introduced in O'Connell et al. (2012) which is based on the distribution locational marginal prices to solve the congestion problems controlling the price values at different nodes. The analysis is extended in Li et al. (2014) to consider the inter-temporal characteristics of the flexible load. Tariff structure for distribution system with DG was proposed in Sooraj and Kumar (2015).

The nodal price behavior considering the ZIP and RIC loads, is considered in Sotkiewicz and Vignolo (2007) with the load flow based formulation. An optimal power flow based approach for distribution system nodal prices with seasonal load impact was presented in Piolliseti and Kumar (2016). However, the impact of renewable energy with its cost was not considered.

2. Mathematical formulation

In this section, an optimization model for determination of nodal prices is proposed with wind integration into the distribution network.

2.1 Optimal power flow model for nodal price: Optimal power flow (OPF) is formulated by minimizing the cost of power at substation and wind power cost which is given by the Equations (1- 7). The objective function includes the total operational cost of substation power and wind power cost function.

Minimize

$$\sum_i (a_i P_{Gi}^2 + b_i P_{Gi} + c_i) + (a_{wi} P_{wi}^2 + b_{wi} P_{wi} + c_{wi}) \tag{1}$$

Subject to

Load flow equations:

$$P_{Gi} - P_{Di} + P_{wi} = V_i \sum_{j=1}^n V_j (G_{ij} \cos \theta_{ij} + B_{ij} \sin \theta_{ij}), \quad i \in S_B \tag{2}$$

$$Q_{Ri} - Q_{Di} + Q_{wi} = V_i \sum_{j=1}^n V_j (G_{ij} \sin \theta_{ij} - B_{ij} \cos \theta_{ij}), \quad i \in S_B \tag{3}$$

Power generation limits, voltage limits and flow limits:

$$P_{Gi}^{min} \leq P_{Gi} \leq P_{Gi}^{max}, \quad i \in S_G \tag{4}$$

$$Q_{Ri}^{min} \leq Q_{Ri} \leq Q_{Ri}^{max}, \quad i \in S_R \tag{5}$$

$$V_i^{min} \leq V_i \leq V_i^{max}, \quad i \in S_B \tag{6}$$

$$|P_l| = |P_{ij}| = |V_i V_j (G_{ij} \cos \theta_{ij} + B_{ij} \sin \theta_{ij}) - V_i^2 G_{ij}| \leq P_l^{max}, \quad l \in S_L \tag{7}$$

where S_B, S_G, S_R and S_L represents the set of nodes, generators, reactive power sources and lines respectively. The voltages, generated real power, generated reactive power, real power demand and reactive power demand are represented by $V_i, P_{Gi}, Q_{Ri}, P_{Di}$ and Q_{Di} . θ_i is the angle at node i , where as G_{ij} and B_{ij} are the real and imaginary parts of the admittance of line connected between i and j nodes, P_l^{max} is the maximum power flow limit in line l . Here P_{wi} is the output power from the wind turbine generator.

Here the values of operational cost coefficients are taken as $a_i=0.01, b_i=40, c_i=9$ and the wind cost coefficients (De Oliveira-De Jesus and Ponce de Leao, 2005) are $a_{wi} = 0.0027, b_{wi}=17.83, c_{wi}=4.46$.

2.2 Nodal price for distribution network: Nodal prices for distribution system can be derived using Marginal Loss Coefficients (MLCs) to get price at each node of the distribution system. MLCs are coefficients which indicate the marginal or incremental deviation in total active power loss due to the changes in active and reactive power injections at a particular node of the system. The active and reactive power MLCs are:

$$\rho_{Pi} = \frac{\partial L}{\partial P_i} \tag{8}$$

$$\rho_{Qi} = \frac{\partial L}{\partial Q_i} \tag{9}$$

where

L : The total power loss

ρ_{Pi} : The active power MLC at node i of the system

ρ_{Qi} : The reactive power MLC at node i of the system

The power supply point (PSP) is defined as the connection between transmission and distribution systems. The price at PSP is indicated by (USD/MWh) which depends on solution of optimal power flow and is given by the following relation.

$$\lambda = 2a_i P_{Gi} + b_i \tag{10}$$

Nodal prices for active and reactive power at all nodes can be found by using following relations

$$N_{Pi} = \lambda (1 + \rho_{Pi}) \tag{11}$$

$$N_{Qi} = \lambda \rho_{Qi} \tag{12}$$

where N_{Pi} (\$/MWh) and N_{Qi} (\$/MVARh) are the active and reactive power nodal prices at node i of the system respectively. The reactive power price at PSP is taken as zero.

2.3 Determination of marginal loss coefficients: The active and reactive power Marginal Loss Coefficients (MLCs) are determined using the Jacobian matrix method. This method of determining the MLCs was proposed by the authors in (De Oliveira-De Jesus and Ponce de Leao, 2005). The following sets of linear equations are utilized in this method.

$$\begin{bmatrix} \rho_{Pi} \\ \rho_{Qi} \end{bmatrix} = \begin{bmatrix} \frac{\partial P_1 \partial P_2}{\partial \theta_1 \partial \theta_1} & \dots & \frac{\partial P_n}{\partial \theta_1} & \frac{\partial Q_1 \partial Q_2}{\partial \theta_1 \partial \theta_1} & \dots & \frac{\partial Q_n}{\partial \theta_1} \\ \vdots & \ddots & \vdots & \vdots & \ddots & \vdots \\ \frac{\partial P_1 \partial P_2}{\partial \theta_n \partial \theta_n} & \dots & \frac{\partial P_n}{\partial \theta_n} & \frac{\partial Q_1 \partial Q_2}{\partial \theta_n \partial \theta_n} & \dots & \frac{\partial Q_n}{\partial \theta_n} \\ \frac{\partial P_1 \partial P_2}{\partial V_1 \partial V_1} & \dots & \frac{\partial P_n}{\partial V_1} & \frac{\partial Q_1 \partial Q_2}{\partial V_1 \partial V_1} & \dots & \frac{\partial Q_n}{\partial V_1} \\ \vdots & \ddots & \vdots & \vdots & \ddots & \vdots \\ \frac{\partial P_1 \partial P_2}{\partial V_n \partial V_n} & \dots & \frac{\partial P_n}{\partial V_n} & \frac{\partial Q_1 \partial Q_2}{\partial V_n \partial V_n} & \dots & \frac{\partial Q_n}{\partial V_n} \end{bmatrix}^{-1} \begin{bmatrix} \frac{\partial L}{\partial \theta_1} \\ \vdots \\ \frac{\partial L}{\partial \theta_n} \\ \frac{\partial L}{\partial V_1} \\ \vdots \\ \frac{\partial L}{\partial V_n} \end{bmatrix} \quad (13)$$

$$\frac{\partial P_i}{\partial \theta_j} = V_i V_j [G_{ij} \sin(\theta_i - \theta_j) - B_{ij} \cos(\theta_i - \theta_j)] \quad (14)$$

$$\frac{\partial P_i}{\partial \theta_i} = -B_{ii} V_i^2 - \sum_{j=1}^n V_i V_j [G_{ij} \sin(\theta_i - \theta_j) - B_{ij} \cos(\theta_i - \theta_j)] \quad (15)$$

$$\frac{\partial P_i}{\partial V_j} = V_i [G_{ij} \cos(\theta_i - \theta_j) + B_{ij} \sin(\theta_i - \theta_j)] \quad (16)$$

$$\frac{\partial P_i}{\partial V_i} = G_{ii} V_i + \sum_{j=1}^n V_j [G_{ij} \cos(\theta_i - \theta_j) + B_{ij} \sin(\theta_i - \theta_j)] \quad (17)$$

$$\frac{\partial Q_i}{\partial \theta_j} = -V_i V_j [G_{ij} \cos(\theta_i - \theta_j) + B_{ij} \sin(\theta_i - \theta_j)] \quad (18)$$

$$\frac{\partial Q_i}{\partial \theta_i} = -G_{ii} V_i^2 + \sum_{j=1}^n V_i V_j [G_{ij} \cos(\theta_i - \theta_j) + B_{ij} \sin(\theta_i - \theta_j)] \quad (19)$$

$$\frac{\partial Q_i}{\partial V_j} = V_i [G_{ij} \sin(\theta_i - \theta_j) - B_{ij} \cos(\theta_i - \theta_j)] \quad (20)$$

$$\frac{\partial Q_i}{\partial V_i} = -B_{ii} V_i + \sum_{j=1}^n V_j [G_{ij} \sin(\theta_i - \theta_j) - B_{ij} \cos(\theta_i - \theta_j)] \quad (21)$$

The total loss of the distribution system is given by

$$L = \frac{1}{2} \sum_{i=1}^n \sum_{j=1}^n G_{ij} [V_i^2 + V_j^2 - 2V_i V_j \cos(\theta_i - \theta_j)] \quad (22)$$

From this equation, the derivative of loss with respect to voltage angles and magnitudes can be derived as follows:

$$\frac{\partial L}{\partial \theta_i} = 2 \sum_{j=1}^n V_i V_j G_{ij} \sin(\theta_i - \theta_j) \quad (23)$$

$$\frac{\partial L}{\partial V_i} = 2 \sum_{j=1}^n G_{ij} [V_i - V_j \cos(\theta_i - \theta_j)] \quad (24)$$

where

V_i, V_j : The voltage magnitudes at the sending and receiving end nodes respectively

θ_i, θ_j : The voltage angles at the sending and receiving end nodes respectively

G_{ij} : The conductance of the $i - j^{th}$ element of the Y-bus matrix

B_{ij} : The susceptance of the $i - j^{th}$ element of the Y-bus matrix

n : The total number of nodes in the system.

2.4 Reconciliated Marginal Loss Coefficients: The approximate total losses of the system can also be obtained from the MLCs as follows:

$$L_{approx} = \sum_{i=1}^n [\rho_{Pi} \cdot P_i + \rho_{Qi} \cdot Q_i] \quad (25)$$

where P_i and Q_i are the active and reactive power injections at node i respectively. As concluded by authors in De Oliveira-De Jesus and Ponce de Leao (2005), it was observed that the value of losses approximated using MLCs were almost as twice as the actual losses of the system. This leads to over estimation of the nodal prices of the system. Hence, the MLCs have to be adjusted in order to estimate the exact cost of losses, which is done using the factor of reconciliation (Rf).

$$Rf = \frac{L}{L_{approx}} \quad (26)$$

With the application of reconciliation, the new active and reactive nodal prices are obtained as shown below:

$$N_{Pi} = \lambda + \lambda \cdot Rf \cdot \rho_{Pi} = \lambda(1 + Rf \cdot \rho_{Pi}) \quad (27)$$

$$N_{Qi} = \lambda \cdot Rf \cdot \rho_{Qi} \quad (28)$$

3. Optimal location for Wind turbine power source

Sensitivity based indices have been used in the recent past to obtain the optimum location for placing the DGs in the distribution system. In this thesis, voltage sensitivity index (VSI) has been utilized to obtain the most optimum location for wind turbine placement in the system.

3.1 Voltage Sensitivity Index (VSI) (Murthy and Kumar, 2014): Sensitivity based indices have been used in the recent past to obtain the optimum location for placing the DGs in the distribution system. In this thesis, voltage sensitivity index (VSI) has been utilized to obtain the most optimum location for wind turbine placement in the system. Voltage sensitivity index is a numerical solution in which the operator knows how close the system is to collapse, the lower the sensitivity index, the closer the bus to collapse hence in this method the bus with low sensitivity is selected for the placement of capacitor. Voltage sensitivity index of bus i is given as follows

$$VSI_i = \sqrt{\frac{\sum_{k=1}^n (1-V_k)^2}{n}} \quad k \in S_B, \tag{29}$$

VSI_i is calculated by placing a DG with the size equal to 25% of the total feeder loading at node i .

Figure 3 shows the voltage sensitivity index profile for the considered 33 bus test system, in which bus 18 is having highest voltage sensitivity index hence this method indicates the bus 18 is the optimal location for wind based DG placement 33 bus radial system.

Using the Weibull parameters, a large number of wind samples which are Weibull distributed can be produced using Monte Carlo simulation (MCS). Since the relationship between wind speed and power production is known from Equation (20), a large number of power samples can also be obtained. The number of samples of MCS is usually more than 10000. Hence, the number of wind power scenarios to be applied to the distribution system is also of the same order. Such a large number of scenarios make the analysis a tasking one. In order to reduce the computational burden of the program developed, the number of scenarios is reduced using a process known as wind speed leveling. The wind turbine will operate from cut-in speed to the cut-out speed specified. The entire range of wind speed from the cut-in speed to the cut-out speed is known as the operating range of the wind turbine. The number of wind speed samples can be grouped into various wind speed ranges specified. Each wind speed sample from the Weibull distribution function will be falling within any one of the wind speed ranges or levels specified.

The wind speed is divided into various levels and power outputs of each level are obtained. The wind speed samples are clustered into levels of wind speeds. Hence, the power outputs corresponding to these wind speeds are also clustered according to wind speed levels. The mean value of power output of each wind speed level is calculated. Then, the probability of occurrence of every wind speed level is calculated by Equation (30).

$$prob_j = \frac{NW_j}{TW} \tag{30}$$

where $prob_j$ is the probability of occurrence of wind speed level j , NW_j is the number of wind speed samples in level j and TW is the total number of wind speed samples. The mean power output of each wind level is multiplied by the probability of occurrence of that level to get that actual wind turbine output for that level. This will provide an accurate representation of the actual wind power output for that wind speed range. The procedure of wind speed levelling is shown graphically in Figure 1.

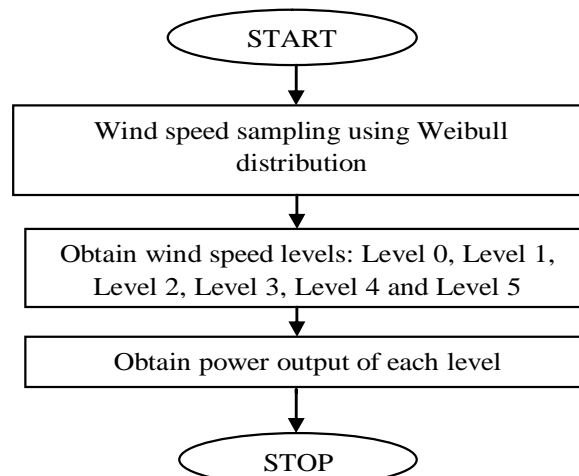


Figure1. Wind speed sampling and leveling

4. Results and discussion

The studies were conducted on the IEEE 33 bus radial and mesh distribution system. The base power of the system is 100 MVA and the base voltage is 12.66 KV. The total connected active power load is 3.72 MW and reactive power load is 2.30 MVAR. An optimal nodal pricing has been obtained considering the seasonal loads, ZIP load and RIC load with the integration of wind energy.

The specifications of the wind turbine selected and the Weibull parameters are given in Murthy and Kumar (2014). From the Weibull parameters, the samples of wind speed are obtained using MCS based sampling. Figure 2 shows a comparison of the scatter diagrams of wind speed vs power output curve of linear and quadratic models.

Table1. Parameter of Wind turbine

Rated Power (P_r in MW)	Cut-in speed (v_{ci} in m/s)	Rated speed (v_r in m/s)	Cut-out speed (v_{co} in m/s)	Shape parameter (k)	Scale parameter (c in m/s)
2.00	3	11.5	20	1.75	8.78

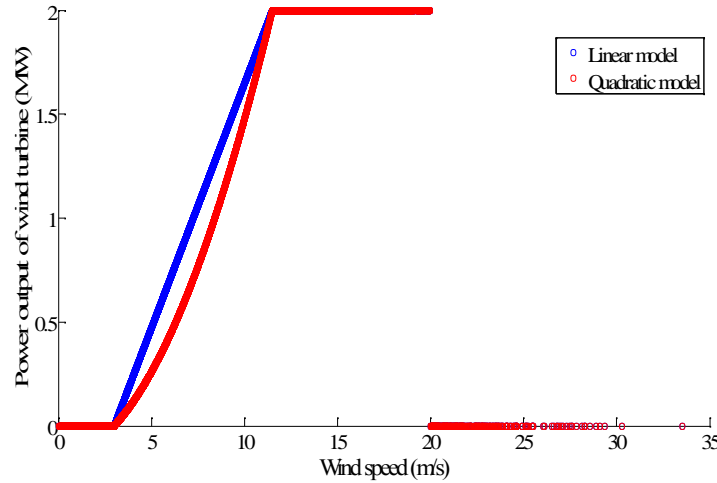


Figure2. Comparison of scatter diagrams of wind speed vs power output of linear and quadratic model

4.1 Levels of Wind Speed

The number of wind speed levels is chosen as five. The wind speed levels and the corresponding speed range are shown in Table 2. Level 0 corresponds to the base case where no wind turbine is integrated. The results obtained in the further sections are obtained using the linear power model discussed in the previous sections.

Table 2. Wind speed levels and the corresponding power outputs

Level index	Speed range (m/s)	Mean power output (MW)	Percentage of rated turbine power output (%)	Probability of occurrence	Actual power output (MW)	Penetration level (%)
0	0-3	0	0	0.1416	0	0.0000
1	3-5	0.2408	12.0399	0.1683	0.0405	1.0887
2	5-8	0.8108	40.5411	0.2636	0.2137	5.7446
3	8-11.5	1.5564	77.8208	0.225	0.3502	9.4139
4	11.5-15	2	100	0.1219	0.2437	6.5510
5	15-20	2	100	0.0654	0.1307	3.5134

For the test system in consideration, Voltage sensitivity index (VSI) values are calculated for zero wind power generation with the proposed OPF. Figure 3 shows the variation of VSI values with bus number. The highest VSI value of 0.0129 is obtained for bus number 18, indicating that the DG should be placed at bus number 18.

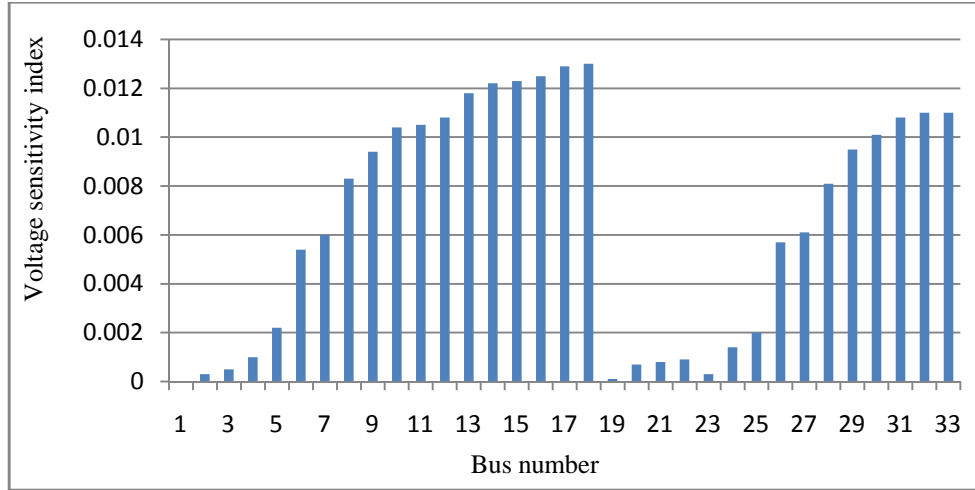


Figure3. Voltage sensitivity index(VSI) values for the nodes of 33 bus RDS

Table 3 shows the comparison of total active power loss (TPL) and the total reactive power loss (TQL) of the 33 bus RDS for various scenarios of wind turbine integration. Table 3 show the branch real power losses for the radial system when the wind turbine is placed at bus 18 for both CP and realistic ZIP loads.

Table 3. Comparison of TPL and TQL for various scenarios of wind turbine placement

Level index	Wind turbine placed at bus number 18 with CP load		Wind turbine placed at bus number 18 with ZIP load	
	TPL (kW)	TQL (kVAR)	TPL (kW)	TQL (kVAR)
0	140.9077	105.9969	131.4810	98.8677
1	136.085	102.1101	131.4338	98.5986
2	118.9697	88.5825	114.7703	85.436
3	109.2605	81.2553	105.3886	78.3728
4	116.5596	86.7284	112.4333	83.6412
5	126.4778	94.4531	122.0666	91.1359

Table 4. Nodal prices for radial system at wind level 3

Bus no:	N _{pi} (\$/MWh)		N _{Qi} (\$/MVARh)		Bus no:	N _{pi} (\$/MWh)		N _{Qi} (\$/MVARh)	
	Without wind	With wind level3	Without wind	With wind level3		Without wind	With wind level3	Without wind	Without wind level 3
1	40.0771	40.0695	0	0	18	43.1824	41.6653	2.2922	1.1491
2	40.0818	40.0723	0.0024	0.0014	19	40.0976	40.0853	0.0176	0.0139
3	40.1063	40.0871	0.0151	0.0092	20	40.2117	40.1784	0.1207	0.0981
4	40.3782	40.2717	0.1590	0.1066	21	40.2292	40.1927	0.1408	0.1145
5	40.7355	40.5229	0.3406	0.2343	22	40.2427	40.2038	0.1587	0.1291
6	41.3943	40.9921	0.9230	0.6481	23	40.1758	40.1439	0.0636	0.0487

Table 4 (cont'd). Nodal prices for radial system at wind level 3

Bus no:	N _{pi} (\$/MWh)		N _{Qi} (\$/MVARh)		Bus no:	N _{pi} (\$/MWh)		N _{Qi} (\$/MVARh)	
	Without wind	With wind level3	Without wind	With wind level3		Without wind	With wind level3	Without wind	Without wind level 3
7	41.4208	41.0094	0.9937	0.6938	24	40.4120	40.3367	0.2511	0.2019
8	42.0058	41.3281	1.4172	0.9239	25	40.5330	40.4355	0.3440	0.2778
9	42.2866	41.4598	1.6156	1.0172	26	41.4989	41.0748	0.9576	0.6785
10	42.5509	41.5758	1.8025	1.0993	27	41.6285	41.179	1.0239	0.7317
11	42.6036	41.5942	1.8185	1.105	28	42.0487	41.5159	1.3993	1.0328
12	42.6950	41.6227	1.8488	1.1144	29	42.3628	41.7678	1.6710	1.2506
13	42.9593	41.7084	2.0580	1.182	30	42.5521	41.9198	1.7645	1.3257
14	43.0204	41.728	2.1376	1.2076	31	42.6977	42.0364	1.9081	1.4408
15	43.0380	41.7368	2.1529	1.2154	32	42.7254	42.0586	1.9395	1.4659
16	43.1014	41.7227	2.1991	1.2052	33	42.7314	42.0634	1.9487	1.4733
17	43.1553	41.7024	2.2712	1.1783					

Table 5. N_{pi} values for various levels with wind turbine

Line no:	w/o Wind	Level 1	Level 2	Level 3	Level 4	Level 5
1	40.0771	40.0762	40.0724	40.0695	40.0718	40.0742
2	40.0818	40.0801	40.0756	40.0723	40.0748	40.0777
3	40.1063	40.1007	40.0924	40.0871	40.0911	40.0961
4	40.3782	40.3328	40.2942	40.2717	40.2887	40.3112
5	40.7355	40.6388	40.5649	40.5229	40.5544	40.5973
6	41.3943	41.2039	41.0676	40.9921	41.0487	41.1271
7	41.4208	41.2264	41.0867	41.0094	41.0673	41.1477
8	42.0058	41.7152	41.4704	41.3281	41.4355	41.5783
9	42.2866	41.9469	41.6409	41.4598	41.5968	41.7761
10	42.5509	42.1639	41.7961	41.5758	41.7428	41.959
11	42.6036	42.2065	41.8241	41.5942	41.7686	41.9936
12	42.695	42.2801	41.8704	41.6227	41.8108	42.0522
13	42.9593	42.4929	42.006	41.7084	41.9347	42.2224
14	43.0204	42.542	42.037	41.728	41.963	42.2615
15	43.038	42.5565	42.0479	41.7368	41.9734	42.274
16	43.1014	42.6028	42.058	41.7227	41.978	42.3005
17	43.1553	42.6411	42.061	41.7024	41.9756	42.3194
18	43.1824	42.6565	42.0452	41.6653	41.9549	42.3177
19	40.0976	40.0939	40.0888	40.0853	40.0879	40.0911
20	40.2117	40.1933	40.1834	40.1784	40.1821	40.1877

Table 5 (cont'd). Npi values for various levels with wind turbine

Line no:	w/o Wind	Level 1	Level 2	Level 3	Level 4	Level 5
21	40.2292	40.2086	40.1979	40.1927	40.1965	40.2025
22	40.2427	40.2204	40.2092	40.2038	40.2077	40.214
23	40.1758	40.1613	40.1501	40.1439	40.1485	40.155
24	40.412	40.3671	40.346	40.3367	40.3434	40.3549
25	40.533	40.4726	40.4464	40.4355	40.4432	40.4573
26	41.4989	41.2947	41.1526	41.0748	41.133	41.2146
27	41.6285	41.4075	41.2591	41.179	41.2388	41.3236
28	42.0487	41.7729	41.6039	41.5159	41.5811	41.6769
29	42.3628	42.0461	41.8616	41.7678	41.837	41.941
30	42.5521	42.2107	42.017	41.9198	41.9914	42.1002
31	42.6977	42.3373	42.1364	42.0364	42.1099	42.2225
32	42.7254	42.3614	42.1591	42.0586	42.1325	42.2458
33	42.7314	42.3666	42.164	42.0634	42.1374	42.2508

Table 6. Nqi values for various levels with wind turbine Normal (CP) load in radial system

Line no:	w/o Wind	Level 1	Level 2	Level 3	Level 4	Level 5
1	0	0	0	0	0	0
2	0.0024	0.002	0.0016	0.0014	0.0016	0.0018
3	0.0151	0.0127	0.0104	0.0092	0.0101	0.0114
4	0.1590	0.1355	0.117	0.1066	0.1144	0.1251
5	0.3406	0.291	0.2546	0.2343	0.2495	0.2705
6	0.9230	0.7905	0.6983	0.6481	0.6856	0.7384
7	0.9937	0.8503	0.7489	0.6938	0.735	0.793
8	1.4172	1.204	1.0263	0.9239	1.0011	1.1044
9	1.6156	1.3677	1.1469	1.0172	1.1153	1.2443
10	1.8025	1.5213	1.2568	1.0993	1.2186	1.3737
11	1.8185	1.5343	1.2654	1.105	1.2266	1.3844
12	1.8488	1.5586	1.2807	1.1144	1.2405	1.4038
13	2.0580	1.727	1.3877	1.182	1.3383	1.5383
14	2.1376	1.791	1.4283	1.2076	1.3754	1.5893
15	2.1529	1.8036	1.4378	1.2154	1.3845	1.6002
16	2.1991	1.8374	1.4452	1.2052	1.3878	1.6195
17	2.2712	1.8884	1.4493	1.1783	1.3847	1.6447
18	2.2922	1.9005	1.4369	1.1491	1.3685	1.6434
19	0.0176	0.0153	0.0143	0.0139	0.0141	0.0147
20	0.1207	0.1051	0.0998	0.0981	0.0992	0.102
21	0.1408	0.1226	0.1165	0.1145	0.1158	0.119
22	0.1587	0.1382	0.1313	0.1291	0.1306	0.1341
23	0.0636	0.0549	0.0506	0.0487	0.0501	0.0524

Table 6 (cont'd). Nqi values for various levels with wind turbine Normal (CP) load in radial system

Line no:	w/o Wind	Level 1	Level 2	Level 3	Level 4	Level 5
24	0.2511	0.2184	0.2062	0.2019	0.2048	0.2112
25	0.3440	0.2994	0.2833	0.2778	0.2815	0.2898
26	0.9576	0.8209	0.7285	0.6785	0.7158	0.7686
27	1.0239	0.8785	0.7829	0.7317	0.7698	0.8244
28	1.3993	1.2051	1.0909	1.0328	1.0757	1.14
29	1.6710	1.4413	1.3138	1.2506	1.2971	1.3684
30	1.7645	1.5226	1.3906	1.3257	1.3733	1.447
31	1.9081	1.6475	1.5083	1.4408	1.4902	1.5677
32	1.9395	1.6748	1.5341	1.4659	1.5158	1.5941
33	1.9487	1.6828	1.5416	1.4733	1.5233	1.6019

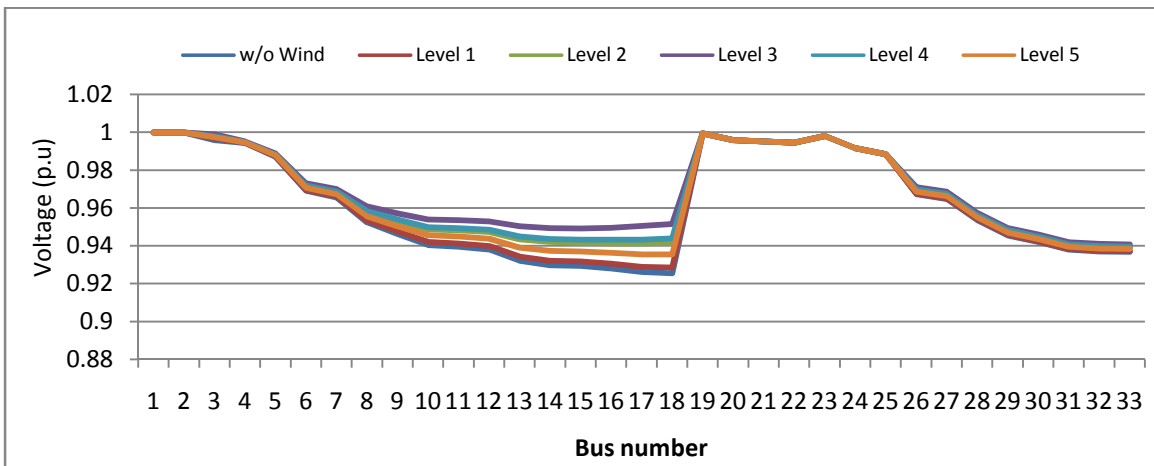


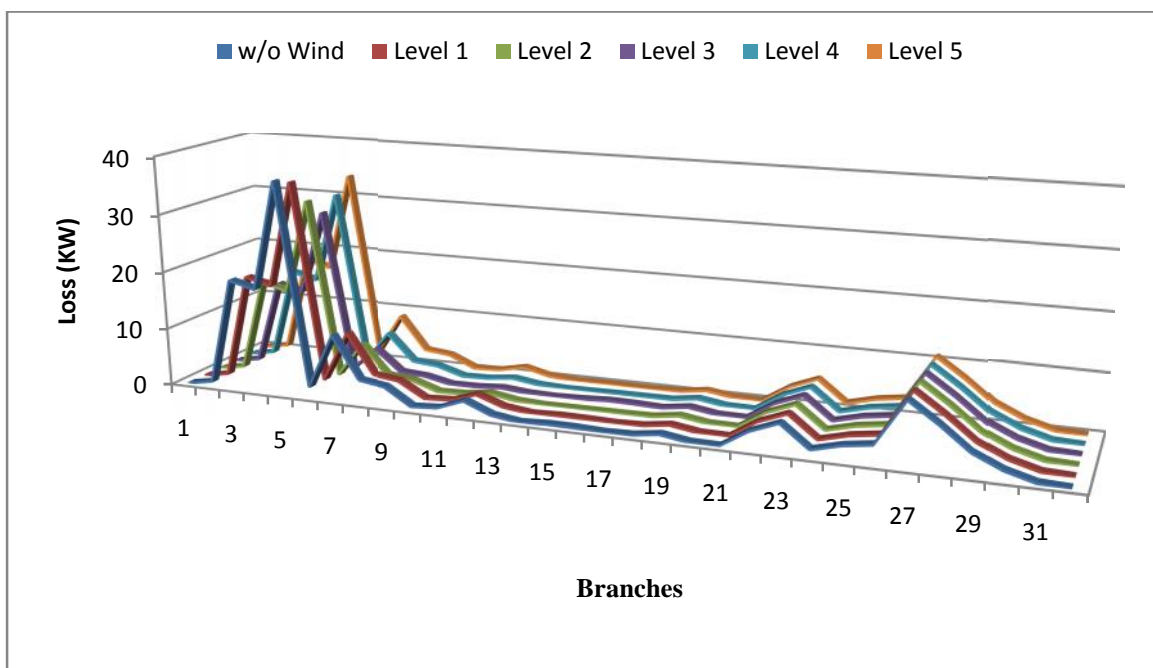
Figure4. Voltage profile for various levels with wind turbine placed at bus 18 with CP load in radial system

Table 4 shows the active and reactive power nodal prices with and without wind integration at wind level 3. As at wind level 3, the losses are observed minimum. The power output of the wind turbine is more compared to other levels. Tables 5 and 6 show the comparison of active and reactive power nodal prices for various scenarios of wind power available in the system. From these results, it can be observed that the active and reactive power losses get reduced with the integration of wind turbines. The TPL for level 0, or without the integration of wind turbine, is 140.9077 kW. Similarly, the TQL for level 0 is 105.9969 kVAR. These values are significantly reduced by placing the wind turbines. For example, the value of TPL after placing wind turbine reduces to a minimum of 109.2605 kW when the wind turbine is placed at bus 18. The value of TQL after placing wind turbine reduces to a minimum of 81.2553 kVAR when the wind turbine is placed at bus 18. For ZIP load, the TPL for level 0, or without the integration of wind turbine, is 131.4810 kW. Similarly, the TQL for level 0 is 98.8677 kVAR. These values are reduced to 105.3886 kW and 78.3728 kVAR respectively. Among all scenarios level3 is giving better results due to its high power output. So, all the results compared below were taken for level 3 scenario. Voltage profile with wind level is shown in Figure 4. It is observed that with wind integration, the voltage profile has improved.

The wind power output for different speed range is given in Table 7. The wind power output, probability of occurrence, and penetration level of the wind power is also given in the table. Loss profile with wind integration is shown in Fig. 5 for all levels of wind power available. It is observed that the branch losses reduce with all levels of wind generation. With reduction in the losses, there is reduction in the marginal loss coefficients and thereby reduction in both the real and reactive power marginal prices.

Table 7. Wind speed levels and the corresponding power outputs

Level index	Speed range (m/s)	Mean power output (MW)	Percentage of rated turbine power output (%)	Probability of occurrence	Actual power output (MW)	Penetration level (%)
0	0-3	0	0	0.1416	0	0.0000
1	3-5	0.2408	12.0399	0.1683	0.0405	1.0887
2	5-8	0.8108	40.5411	0.2636	0.2137	5.7446
3	8-11.5	1.5564	77.8208	0.225	0.3502	9.4139
4	11.5-15	2	100	0.1219	0.2437	6.5510
5	15-20	2	100	0.0654	0.1307	3.5134

**Figure 5.** Branch real power losses for various levels with wind turbine for CP load in radial system

5. Conclusions

In this study, the impacts of wind power integration on the optimal nodal pricing of distribution systems were discussed for radial system. The variability of wind power output is observed to cause noteworthy deviations in the nodal prices of the distribution system. These deviations are important as the volatility of wind power outputs leads to volatility in the nodal prices of the system. There is reduction in the all branches with wind integration and due to reduction in the losses, there is reduction in the marginal loss coefficients and nodal prices. The active and reactive power nodal prices of the distribution system are observed lower with the integration of wind turbines into the system.

References

- De Oliveira-De Jesus P. M., Ponce de Leao M. T., 2005. Cost of loss allocation in distribution networks with high penetration of distributed renewable generation – a comparative study. *International Conference on Renewable Energy and Power Quality, Zaragoza*: 2005.
- Ghayeni. M., Ghazi. R., 2011. Transmission network cost allocation with nodal pricing approach based on ramsay pricing concept. *IET Generation, Transmission & Distribution*, Vol.5, pp. 384-392.
- Li R., Wu Q., Oren S. S., 2014. Distributional locational marginal pricing for optimal electric vehicle charging management. *IEEE Transactions on Power Systems*, Vol. 29, pp. 203-211.
- Murthy V. V. S. N., Kumar A., 2014. Mesh distribution system analysis in presence of distributed generation with time varying load model. *International Journal of Electrical Power & Energy Systems*, Vol.62, pp. 836-854.
- Mutale J., Strbac G., Curcic. S., Jenkins. N., 2000. Allocation of losses in distribution systems with embedded generation. *IEE Proceedings - Generation, Transmission and Distribution*, Vol.147, pp. 7-14.

- O'Connell N., Wu Q., Ostergaard J., Nielsen A. H., Cha S. T., Ding Y. , 2012. Day ahead tariff for the alleviation of distribution grid congestion from electric vehicles. *Electric Power Systems Research*, Vol.92, pp. 106-114.
- Polisetti K., Kumar A., 2016. Distribution system nodal prices determination for realistic ZIP and seasonal loads: An optimal power flow approach. *Procedia Technology*, Vol.25, pp.702-709.
- Singh R. K., Goswami S. K., 2006. Optimal allocation of distributed generations based on nodal pricing for profit, loss reduction and voltage improvement including voltage rise issue. *International Journal of Electrical Power & Energy Systems*, Vol.32, pp. 637-644.
- Sooraj N.K., Kumar A., 2015. Distribution system nodal pricing analysis with realistic ZIP load and variable wind power source. *2015 Annual IEEE India Conference (INDICON)*, DOI: 10.1109/INDICON.2015.7443140.
- Sotkiewicz. P. M., Vignolo J. M., 2007. Towards a cost causation-based tariff for distribution network with DG. *IEEE Transactions on Power Systems*, Vol. 22, pp. 1051-1060.
- Sotkiewicz P. M., Vignolo J. M., 2006. Nodal pricing for distribution networks: efficient pricing for efficiency enhancing DG. *IEEE Transactions on Power Systems*, Vol.21, pp.1013-1014.
- Sotkiewicz P. M., Vignolo J. M., 2012. The value of intermittent wind DG under nodal prices and amp – mile tariffs. *Transmission and Distribution: Latin America Conference and Exposition (T&D-LA), 2012 Sixth IEEE/PES*, pp.1-7.
- Zhao Q., Wang P., Ding Y., Goel L.K., 2010. Impacts of solar power penetration on nodal prices and nodal reliability. *2010 Conference Proceedings IPEC*, pp.1134-1139.
- Zhao Q., Wang P., Goel L., Ding Y., 2011. Impacts of renewable energy penetration on nodal price and nodal reliability in deregulated power system. *IEEE Power and Energy Society General Meeting*, pp.1-6.

Received September 2016

Accepted November 2016

Final acceptance in revised form June 2017